Received October 1997
Revised December 1997
Accepted March 1998

Numerical study of early stages of an impulsively started unsteady laminar flow past expanded trapezoidal cylinders

T.S. Lee
Mechanical and Production Engineering Department, National University of Singapore, Singapore

Nomenclature

a = width of the frontal surface of the trapezoidal cylinder
ADI = Alternating Direction Implicit method
b = width of the aft end surface of the trapezoidal cylinder
Cp = pressure coefficient
Cd = drag coefficient
J = Jacobian matrix
L = characteristic length (L = b)
p = non-dimensional pressure
Re = Reynolds number ($\rho u_0 \cdot L/\mu$)
t = time
TDMA = tridiagonal matrix algorithm
u_ξ = non-dimensional velocity in ξ direction
u_η = non-dimensional velocity in η direction
U = mean velocity at inlet section, the characteristic velocity
V_{max} = maximum nondimensional velocity
ξ = longitudinal co-ordinate in generalized system
η = lateral co-ordinate in generalized system
ν = fluid molecular kinetic viscosity
ψ = stream function
ζ = vorticity

1. Introduction

Studies of flow over cylinders, such as circular cylinders, square cylinders, rectangular cylinders and flat plates are of great importance in many engineering applications. Examples of these applications include the designs of tower structures, suspension bridges, chimneys, heat exchangers, road vehicles, tall buildings, flow meters etc. Few considered the trapezoidal cylinders. Most of the present work on flow over cylinders also focused on long term flow development. Few considered the studies on the early stages of impulsively started flow. The evolution of the separated flow around cylinders at the early stages are known to be very different from the long term wake development. It was generally noted that due to the build-up of fluid in the recirculation zones behind the body prior to the initiation of shedding, the

International Journal of Numerical Methods for Heat & Fluid Flow
Vol. 8 No. 8, 1998, pp. 934-955.

The author gratefully acknowledges the financial assistance of a research grant RP890633 from the National University of Singapore. During the course of this work, the assistance of S.H. Winoto, Y.P. Xu and Ronald Tan are also gratefully acknowledged.

initial vortices that came off were very large followed by some smaller and regularly shaped vortices that appeared once steady-state shedding was reached. Hence, study of the flow development characteristics during the early stages of an impulsively started flow are necessary for the better understanding of the building up of the recirculation zone before the flow burst into smaller Karman type vortices.

For numerical work, Davis and Moore (1982) studied vortex shedding from two-dimensional time-dependent flow past rectangular cylinders. Nagano (1982) investigated similar flow over a rectangular cylinder by the discrete vortex model. Fernando and Modi (1990) used the Boundary Element Method in conjunction with the Discrete Vortex Model to represent the complex unsteady flow field around a bluff body with separating shear layers. Lisa and Balasubramaniam (1993) used a finite element method to investigate the Strouhal frequencies in vortex shedding over square cylinders with surface suction and blowing. Kim and Benson (1992) made a comparison of various numerical methods: the SMAC, PISO and Iterative Time Advancing schemes for unsteady flows past a circular and a square cylinder. The capability of each of the above schemes to solve the unsteady flows was found to be attributed to a pressure correction algorithm that strongly enforces the conservation of mass.

For experimental work, many researchers studied the low Reynolds number flow around circular, rectangular and square cylinders. Bearman and Trueman (1972) carried out flow visualization study of flow over rectangular cylinders. They showed that the drag coefficient was found to be strongly influenced by the presence of the trailing corners. Coutanceau and Bouard (1977) and Bouard and Coutanceau (1980) used flow visualization as their main tool for studying the wakes behind an impulsively started flow past circular cylinders. They were interested in the near wake evaluation. They found that the characteristics of the pair of symmetric standing eddies and the appearance of secondary phenomena near the wake region depend on the initial Reynolds number. The characteristics of the early wake development can have a strong influence on the evaluation of effects of secondary phenomena. Gerrard (1966, 1978) carried out a series of experiments providing very careful flow visualization studies on a circular cylinder in water using a towing tank. At a certain Reynolds number, the length of the recirculation region containing a pair of contra-rotating standing eddies were found approximately two cylinder diameters long. At higher Reynolds numbers, Gerrard observed dye which had rolled up into votes returning towards the cylinder in what he referred to as a “finger”. Gerrard (1978) also observed the three-dimensional nature of the wake flow, as time progress from the initial start-up of the motion, the influence of the ends began to spread across the span and gave rise to bowed vortices. Okajima (1982) and Okajima and Kitajima (1993) investigated the fluid behaviour around square and rectangular cylinders in a wind tunnel and in a water tank. For the cylinders with width to height ratios of 2 and 3, there existed a certain range of Reynolds numbers where the abrupt change of flow pattern occurred with a sudden

discontinuity in the Strouhal-number curves. For the Reynolds number below that region, the flow separated at the leading edges reattached on either the upper or the lower surface during a period of vortex shedding. For Reynolds number beyond it, the flow tended to reattach on the cylinder owing to the increasing effects of the Reynolds stressed and turbulent entertainment at high Reynolds number. More recently, Kyoji and Yoshifumi (1992) visualized water flows over a circular cylinder and a trapezoidal cylinder in a circular pipe in order to investigate the complexity of the flow in a flow-meter. From their experiment, it was shown that the formation of Karman-vortex-like vortices are three-dimensional in nature when forming behind a circular cylinder or a trapezoidal cylinder as the separated shear layer wrapped up the fluid just behind the cylinder. Also, the leading edge of the separation region was observed to move up to a certain distance behind the circular cylinder with the increasing Reynolds number.

2. Governing equations and numerical procedures

Figure 1 shows the geometrical configurations of the flow over an expanded trapezoidal cylinder. Flow over the trapezoidal cylinder can be described by the vorticity transport equation

$$\frac{\partial \bar{\zeta}}{\partial t} - \nabla \times (\bar{u} \times \bar{\zeta}) = \frac{1}{\mathrm{Re}} (\nabla^2 \bar{\zeta}) + S \tag{1}$$

with the vorticity defined as

$$\bar{\zeta} = -\nabla^2 \bar{\psi} \tag{2}$$

and the velocity is given by

$$\bar{u} = \nabla \times \bar{\psi} \tag{3}$$

where $\bar{\zeta}$, $\bar{\psi}$, $\bar{u}$ represent the vorticity; stream function and velocity respectively; S represents the source term. The inflow Reynolds number is defined as Re = $\rho u_0 b / \mu$.

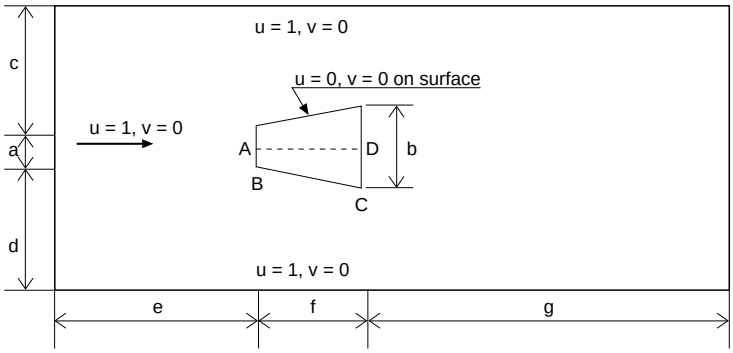

Figure 1.
Problem definition

For the solution domain considered here, a uniform velocity is assumed at the inlet boundary. Normal derivative of the velocity is assumed zero at the outlet boundary. Along the other two horizontal boundaries, the flows are assumed to be sufficiently far from the influence by the presence of the expanded trapezoidal cylinder. Hence, the horizontal velocity component is assumed to be the undisturbed uniform velocity value and the normal velocity component is assumed to be zero. Non-slip conditions are prescribed at the surfaces of the expanded trapezoidal cylinder. The stream function and vorticity boundary conditions follow the relationships given by equation (3) with respect to the specified velocity boundary conditions. The streamline at the axis of symmetry is assigned a reference value of zero.

The present work is concerned only with the initial stages of the impulsively started flow over the expanded trapezoidal cylinder. Thus, the numerical solution is an initial value problem. Besides the boundary conditions specified, the initial velocities, vorticity, pressure and stream function fields must be known at the initial time. At time t = 0, the velocity field is assumed their values at the inlet section (hence, the term “impulsively started flow”). The initial pressure field is set to a reference value of zero.

In the present study, the flow governing equations (1)-(3) are expressed in generalised curvilinear co-ordinate system. This allows the implementation of a numerical scheme on the Cartesian grid where the geometric characters are embedded in the coefficients of the transformed equations. For the two-dimensional problem considered here, the curvilinear equation for the vorticity transport equation can be expressed as

$$J\frac{\partial \zeta}{\partial t}+\frac{J}{\mathrm{Re}}\frac{\partial(\zeta U)}{\partial \xi}+\frac{J}{\mathrm{Re}}\frac{\partial(\zeta V)}{\partial \eta}=\frac{J}{\mathrm{Re}}\frac{\partial(g^{11}\zeta_{\xi}+g^{12}\zeta_{\eta})}{\partial \xi}+\frac{J}{\mathrm{Re}}\frac{\partial(g^{21}\zeta_{\xi}+g^{22}\zeta_{\eta})}{\partial \eta} \quad (4)$$

The non dimensional variables are defined as:

$$u=\frac{\bar{u}}{u_0} \qquad v=\frac{\bar{v}}{v_0} \qquad x=\frac{\bar{x}}{L} \qquad y=\frac{\bar{y}}{L} \qquad t=\frac{\bar{t}}{T_0} \quad (5)$$

where u_0 and L are reference quantities and the over bar denotes a dimensional parameter. In this study, u_0 equals u_∞, L = b is the aft end dimension of the expanded trapezoidal cylinder, $T_0 = L/u_0$ may be interpreted as the time required for the impulsively started flow to move over one cylinder spacing. Thus, t is equivalent to the number of cylinder spacings the flow has moved since its impulsive start at t = 0.

The curvilinear velocity U, V described in equation (4) and the Cartesian velocity components u, v are related by

$$U = u\xi_x + v\xi_y,\ V = u\eta_x + v\eta_y \quad (6)$$

The Jacobian matrix J and the matrix terms ξ_x, ξ_y, η_x, η_y are obtained from

$$\xi_x = \frac{y_\eta}{J},\ \xi_y = -\frac{x_\eta}{J},\ \eta_x = -\frac{y_\xi}{J},\ \eta_y = \frac{x_\xi}{J} \tag{7}$$

and the tensor components are represented by

$$g^{11} = \xi_x^2 + \xi_y^2 \qquad g^{12} = \xi_x\eta_x + \xi_y\eta_y \qquad g^{21} = g^{12} \qquad g^{22} = \eta_x^2 + \eta_y^2 \tag{8}$$

The algorithm of the numerical solution followed closely the Alternating Direction Implicit (ADI) method proposed by Samarskii and Andree (1963). Basically, the advancement over one time step is accomplished through:

$$\left(I - \Delta t A_\xi\right)\left(\bar{\zeta}\right)^* = \left(A_\xi + A_\eta\right)\left(\bar{\zeta}\right)^n + \left(S_D\right)^n$$

$$\left(I - \Delta t A_\xi\right)\left(\bar{\zeta}\right)^{**} = \left(\bar{\zeta}\right)^*$$

$$\left(\bar{\zeta}\right)^{n+1} = \left(\bar{\zeta}\right) + \Delta t\left(\bar{\zeta}\right)^{**} \tag{9}$$

The streamline field is then obtained from the vorticity field through equation (2) by a Successive Over Relaxation (SOR) iteration procedure (Roache, 1972). The velocity fields are obtained from equation (3) and the pressure field is obtained directly from the streamline field:

$$\nabla^2 P = 2\left[\frac{\partial^2\psi}{\partial x^2}\frac{\partial^2\psi}{\partial y^2} - \left(\frac{\partial^2\psi}{\partial x\partial y}\right)^2\right] \tag{10}$$

The present work is concerned only with the initial stages of the impulsively started flow over expanded trapezoidal cylinder. The numerical solution of the impulsively started flow over the expanded trapezoidal cylinder is thus an initial boundary value problem. Besides the boundary conditions specified earlier, the velocities and pressure must be known at the initial time in order to carry out the numerical computation of the unsteady flow.

The boundary conditions for the problem considered here are shown in Figure 1 and the finite difference mesh used in the present study is shown in Figure 2. The location of the cylinder in the computational domain as shown in Figure 1 is determined through a series of preliminary numerical test runs. For a = 1/2b, the optimum parameters obtained are: c = d = 7a, e = 4.5a, g = 14.5a and f = b, where a is the length of the frontal side of the trapezoid, b is the length of the rear side.

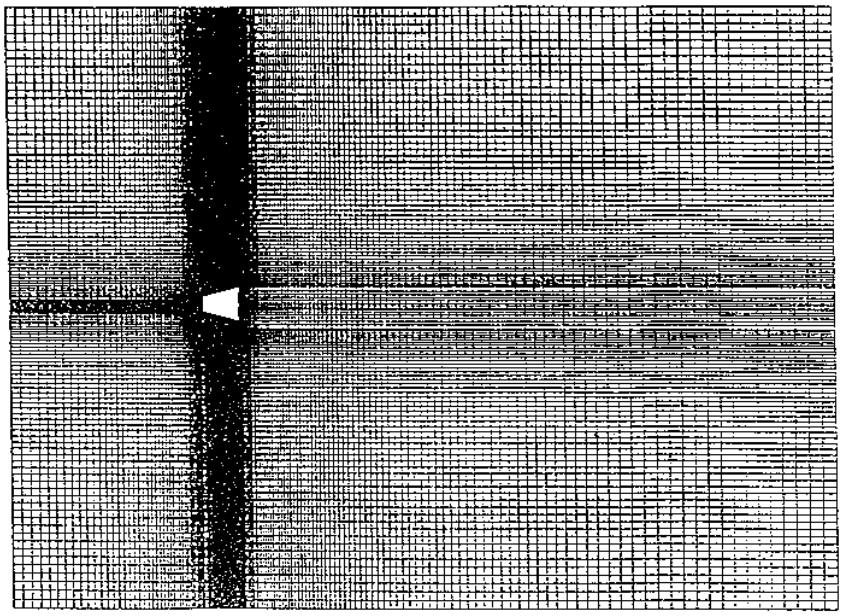

Figure 2.
Finite difference mesh

The distance from the symmetrical axis of the cylinder to the lower and upper sides of the computational domain is chosen to be sufficiently far so as to satisfy the requirement that the solution domain is almost infinite. The finite difference mesh used is shown in Figure 2. Grid independent test has been carried out for an impulsively started flow over the expanded trapezoidal cylinder for all the Reynolds number considered here on grid size of 81×61, 101×101, 161×121 and 181×161. From the results obtained the difference between the grid sizes of 161×121 and 181×161 are negligible. Thus, the total number of grids used in the present calculation is of 161×121. A numerical grid generation procedure was also introduced to provide more grid points near the solid boundary so as to obtain better insight of the fluid phenomena within the wake regions.

3. Results and discussions

For the present analysis of the impulsively started flow over the expanded trapezoidal cylinders, numerical results are presented for time variations of streamline patterns, pressure contours, surface pressure coefficients, drag coefficients and closed wake length of the impulsively started flow over the cylinder. The study are presented here for study of the early stages of symmetrical wake flow developments. The numerical results obtained are for Re = 25, 50, 250, 500 and 1,000. Computations of the symmetrical flow past the expanded trapezoidal cylinder were obtained for short dimensionless time of t = 8.

Figures 3 to 8 show the evolution with time of the impulsively started streamline flow structure over the expanded trapezoidal cylinder for Re = 25, 50, 150, 250, 500 and 1,000 respectively. Immediately after the start of the flow,

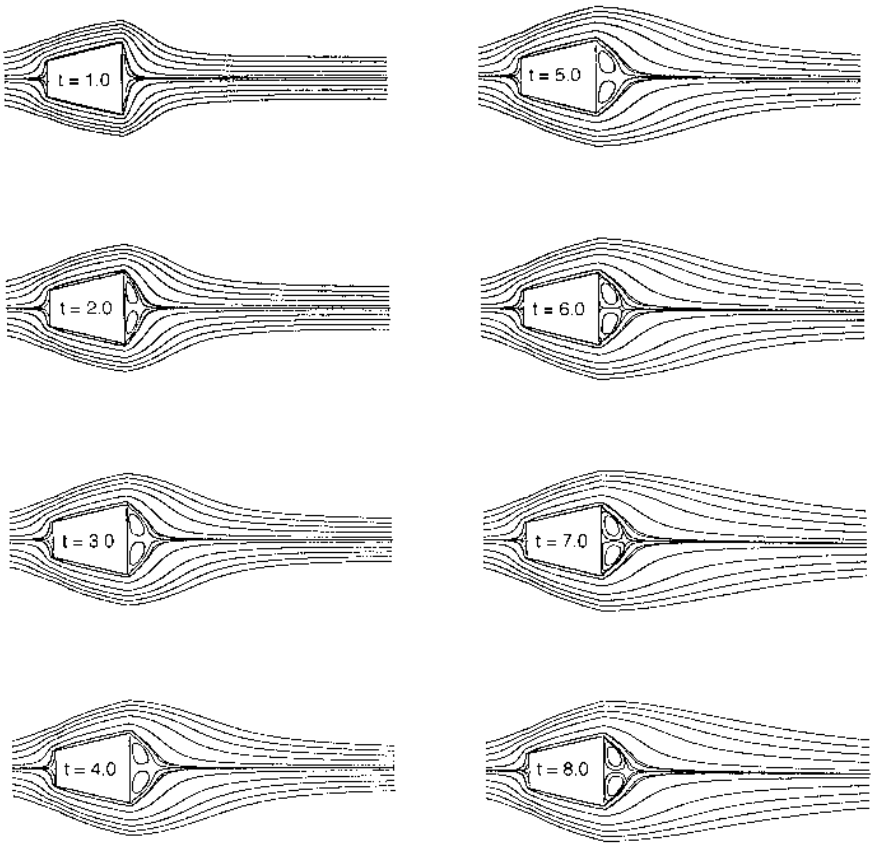

Figure 3.
Instantaneous streamline pattern for Re = 25 at various times

the flow is typically irrotational everywhere [Type I main-flow]. But as the flow moves over the expanded trapezoidal cylinder, vorticity is generated at the solid surface and transported to the region of the rear stagnation point, inducing a reversal flow. This reverse flow in time grows into a symmetrical standing zone of recirculation at the aft end of the cylinder [Type II main-flow]. Flow separation from the leading edges of the expanded trapezoidal cylinder develops insignificantly initially but grows gradually along the upper and lower surfaces of the cylinder as Re increases or when time advances [Type III main-flow]. Above a critical Reynolds number Re_{crit}, and after a critical period of time (t^*) which is shorter as the Reynolds numbers becomes greater, the separated flows from the leading edges of the expanded trapezoidal cylinder merge with the swelling recirculation wake flow region at the aft end of the cylinder. This creates a complex recirculatory flow pattern [Type IV main-flow] with possible tertiary recirculations at the meeting points of the Type II and Type III separated flows. However, the present investigation is limited to cases where the recirculation zones in which eddies develop, remain symmetrical and stably attached to the expanded trapezoidal cylinder.

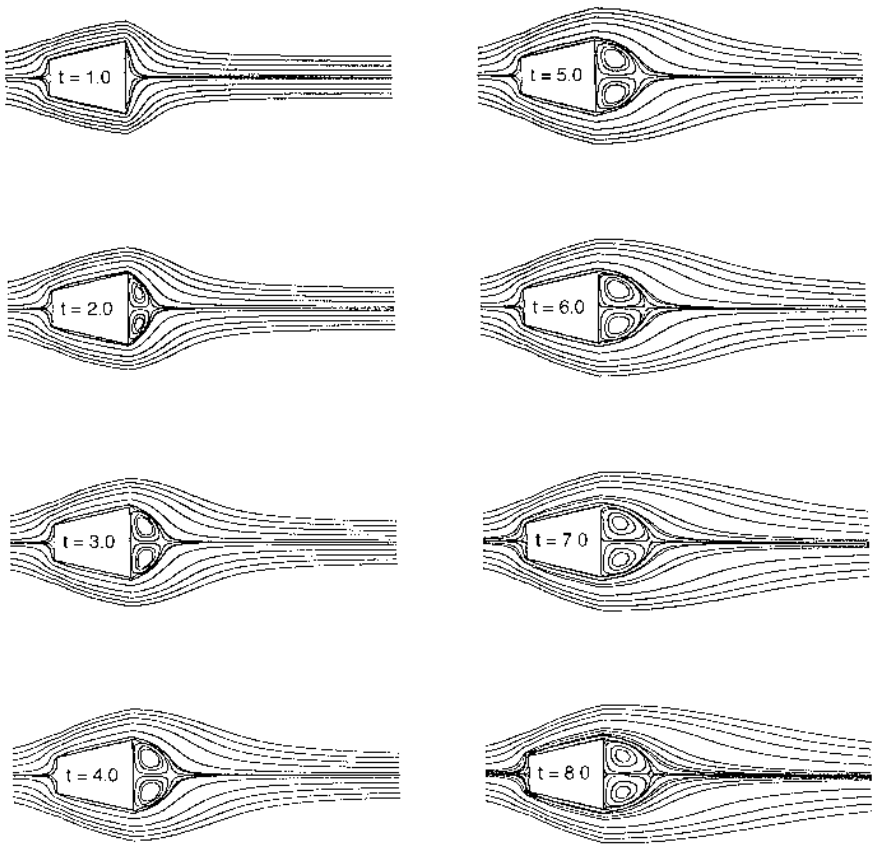

Figure 4.
Instantaneous streamline pattern for Re = 50 at various times

A simple qualitative examination of the developing streamlines contours shows that the time development of the flow differs when Re is increased. With regards to the Reynolds number, it is possible to distinguish three categories of flow time evolution which correspond roughly to small, moderate and high Reynolds numbers where the flow remains symmetrical and attached to the expanded trapezoidal cylinder:

$Re < Re_1$, $Re_1 < Re < Re_2$ and $Re > Re_2$

The exact limiting values of Re_1 and Re_2 cannot be determined by this qualitative investigation; they will be classified subsequently by means of the numerical presentations of the streamline contours on the main characteristics of the flow. However, for the sake of illustration, it can be said that the values of Re_1 and Re_2 have been found to be approximately 50 and 500.

Time evolution at low Reynolds numbers: $Re < Re_1$

If the value of Re remain below the limiting value of Re_1 and the flow time is small ($t < 1.0$), the flow develops with time without visible flow separation and

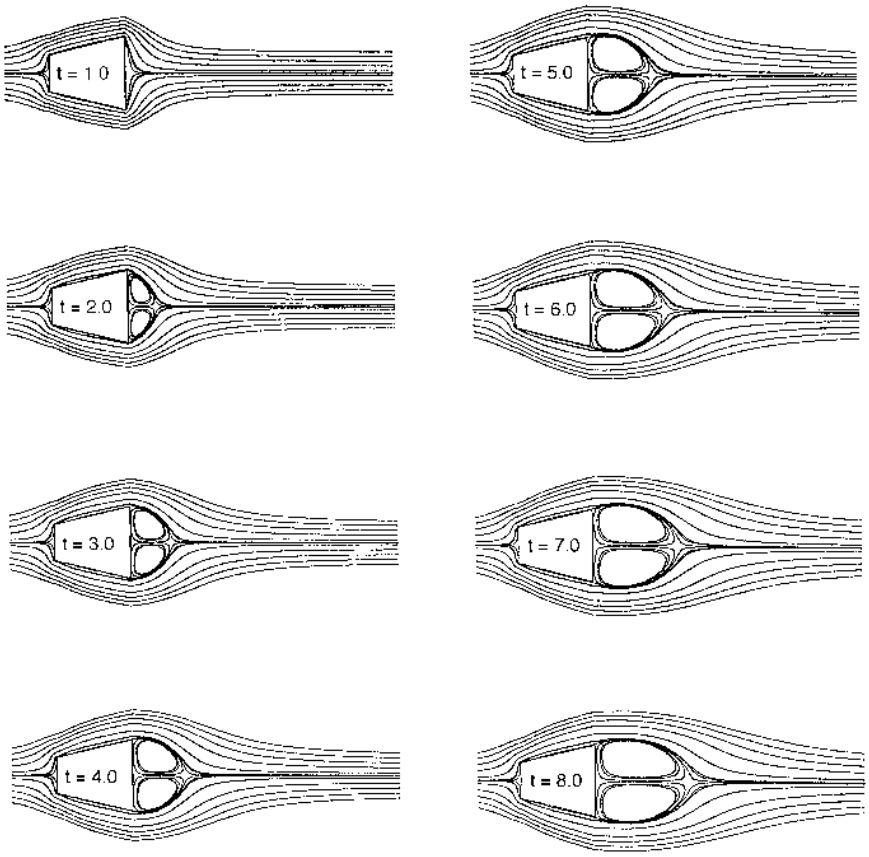

Figure 5.
Instantaneous streamline pattern for Re = 150 at various times

reattachment [Type I main-flow]. After a short lapse of time, the flow separates first from the rear surface of the expanded trapezoidal cylinder [Type II main-flow] and forms aft end symmetrical eddies within a recirculating zone [Sub-flow (a)]. This unique recirculating zone consists typically of the two symmetrical eddies. The size of the recirculating zone is smaller than the aft end dimension of the cylinder. Typical flow pattern for this regime of flow can be visualized in Figures 3 and 4. For Re = 25 (Figure 3), the aft end twin eddies develop as soon as t > 1.5. The length and the width of the recirculation region grow as flow time advances. However, the width of the recirculation region remains smaller than the width of the aft end of the expanded trapezoidal cylinder. Similar flow development can also be seen for Re = 50 (Figure 4).

Time evolution at moderate Reynolds numbers: $Re_1 < Re < Re_2$

As Reynolds number is further increased, the domains of the recirculating zone increase rapidly. Typical for this category of flow, recirculatory flow phenomena begin to appear during the flow development. First, near the

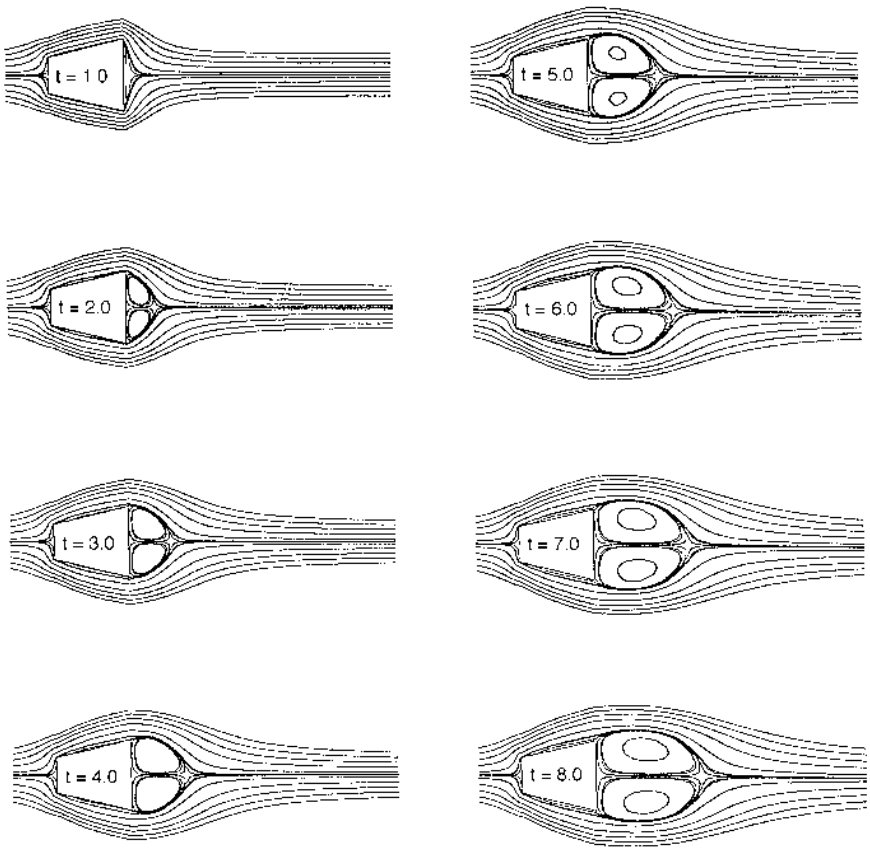

Figure 6.
Instantaneous streamline pattern for Re = 250 at various times

sharp corners at the rear surface of the expanded trapezoidal, the fluid particles passing through this region deviate from the cylinder causing a separation region in the streamline pattern. The recirculation region of the close wake is established. As flow time progresses, the aft end eddies grow larger than the width of the cylinder. Above a critical Reynolds number Re_{crit}, and after a critical period of time (t^*) which is shorter as the Reynolds numbers become greater, the separated flows from the leading edges of the expanded trapezoidal cylinder grow and begin to merge with the growing aft end eddies.This type of flow is typically represented by flows shown in Figures 5 and 6 for Re = 150 and 250 respectively. At Re = 150, Figure 5 shows that for t > 3.0, the separated flow region grows, with its size approaching the width of the aft end cylinder. At t > 5.0, the width and length of the twin eddies are larger than the aft end dimension of the cylinder. The separated flows from the leading edges of the expanded trapezoidal cylinder grow and begin to merge with the growing aft end eddies. Similar flow patterns can be seen in Figure 6.

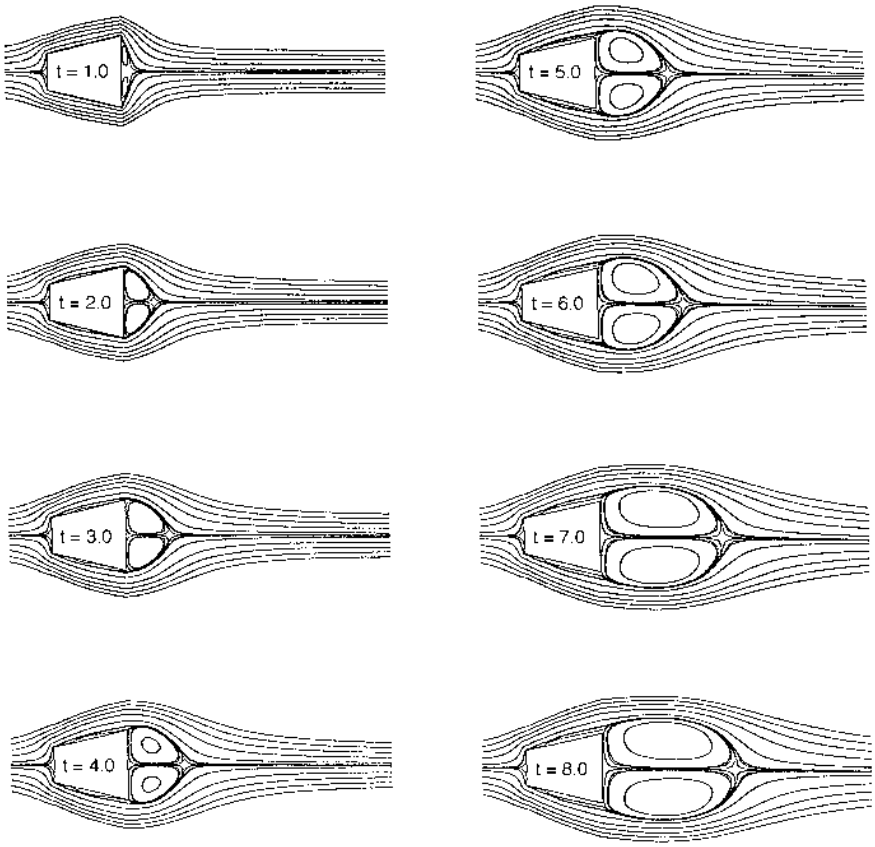

Figure 7.
Instantaneous streamline pattern for Re = 500 at various times

Time evolution at high Reynolds numbers: Re > Re2

Typical flow in this regime can be represented by Figures 7 and 8 with Re = 500 and 1,000 respectively. As flow time advances, the streamlines separating from the leading edges of the upper and lower inclined surfaces of the expanded trapezoidal cylinder [Type III main-flow] merge with the growing recirculation region at the aft end of the cylinder. This results in a complex recirculatory flow pattern [Type IV main-flow] with tertiary disturbances [Sub-flow (c)] near the meeting points between the Type II and Type III flows. The complexity of the flow pattern depends on the Reynolds number. For Re = 500, the twin eddies appear for t > 1.0 near the aft surface of the expanded trapezoidal cylinder. At t = 3.0, the streamlines separate at the leading corners of the expanded trapezoidal cylinder forming minor recirculatory flow regions at the upper and lower inclined surfaces of the cylinder. As time advances, these separated secondary flows move towards the rear end and join up with the recirculating flow in the wake region. A complex tertiary sub-flow region was identified. Similar flow patterns can be observed for Re = 1,000 (Figure 8).

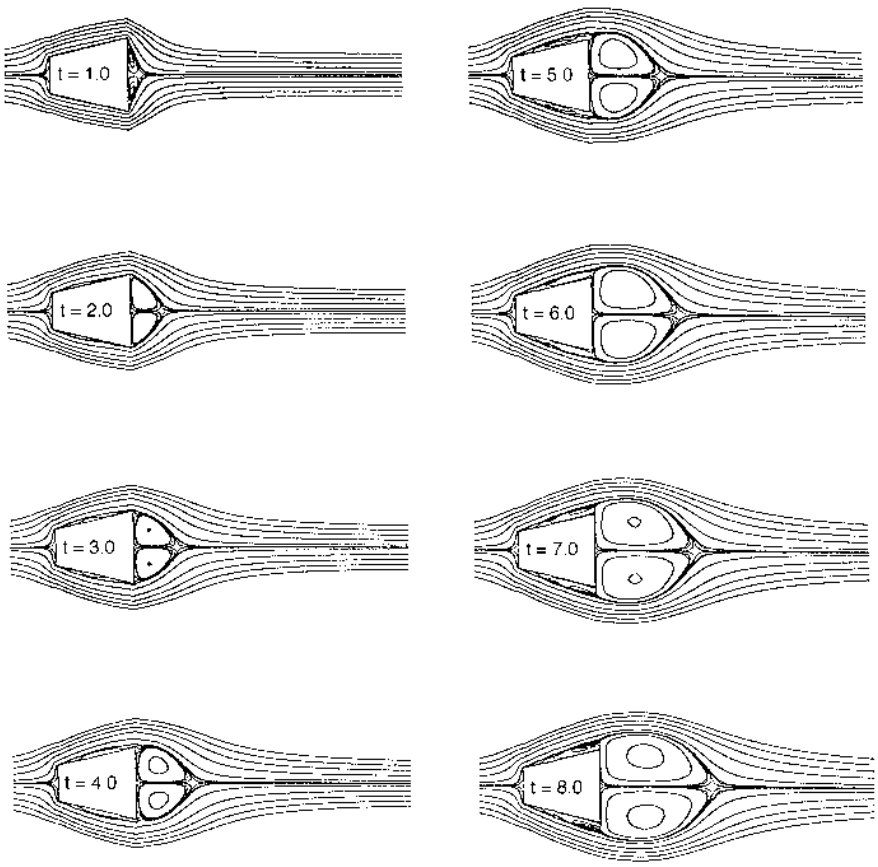

Figure 8.
Instantaneous streamline pattern for Re = 1,000 at various times

It should be pointed out here that for larger values of t, if an external disturbance is introduced, this will lead to vortex shedding. The flow solution may then bifurcate between symmetrical wake and Karman wake. It is also possible that the symmetrical wake at higher Reynolds numbers bifurcates between a steady state configuration and oscillating configuration or a periodic one of a different nature. These are not within the present scope of study.

Evolution of the flow characteristics in the sub-flow regions

Figures 3 to 8 also show the time evolution of the shape and structure of the various type of sub-flows (a), (b) and (c) for different values of the Reynolds number. The recirculation eddies at the aft end of the cylinder [Sub-flow (a)] rotates in the same directions as the eddies at the upper and lower inclined surfaces of the expanded trapezoidal cylinder [Sub-flow (b)]. The flow separation shear layers and the main recirculation zone grow in size both with time and as Reynolds number increases.

For Re = 25, Figure 5 shows typically the time development of the sub-flow (a). They start from the rear cylinder surface without presenting any variation in their concavities and remain smooth until their downstream extremities. It can be seen that in the earlier stage of the flow development the point of reattachment moves very quickly downstream. But from t > 3.0 the evolution becomes slow. At this value of Re, the maximum width of sub-flow (a) remains smaller than the width of the trailing edge of the expanded trapezoidal cylinder. For Re = 50, the outlines of the sub-flow (a) follow closely that for Re = 25 for t < 3.0. The width of the wake remains smaller than the width of the trailing edge of the expanded trapezoidal cylinder.

For Re = 150 and 250, the width of the wake of sub-flow (a) becomes clearly larger than the width of the trailing edge of the expanded trapezoidal cylinder for t > 4.0. The separated flows [Sub-flow (b)] develop from the leading edges of the cylinder and begin to more towards the recirculation zone in the wake region.

For Re = 500 and 1,000, the width of the wake of the sub-flow (a) are larger than the width of the trailing edge of the expanded trapezoidal cylinder for t > 4.0. The separated flows [Sub-flow (b)] develop from the leading edges of the cylinder, move along the upper and lower edges of the cylinder and eventually merge with the growing recirculation zone in the wake region.

In general, the above study shows that for Reynolds numbers greater than a critical value and after a certain time period, separated flows from the leading edges of the expanded trapezoidal cylinder merge with the growing main recirculating zone aft of the cylinder. This creates a tertiary flow regime [Sub-flow (c)] between the two merging recirculatory flows.

Evolution of other characteristics

Having made a comprehensive study by analysing the characteristics of the main recirculatory flow regions, we now consider the other derived characteristics of the flow, namely, the flow field pressure contours, the surface pressure coefficient, the wake length and the drag coefficient.

Figures 9 to 14 show the time variation at t = 2.0, 4.0, 6.0 and 8.0 of the pressure contours for Re = 25, 50, 150, 250, 500 and 1,000 respectively. For the range of Reynolds numbers considered here, the development of the pressure contour lines follow closely the development of the streamline patterns. For Re = 25 and at t = 2.0, the pressure contour indicates that there is little recirculation region present. As time advances, the development of the wake region behind the rear wall of the expanded trapezoidal cylinder can be recognised. From the corresponding streamline patterns for Re = 50, the small vortices can be seen developing from the rear wall causing the pressure contour lines to separate at t = 2.0. The pressure contour lines become closer and eventually merge at t = 8.0. From the outline of the wake region at different time levels, the twin vortices can be seen growing larger and larger as time advances. Figure 11 shows the pressure contours for Re = 150. In

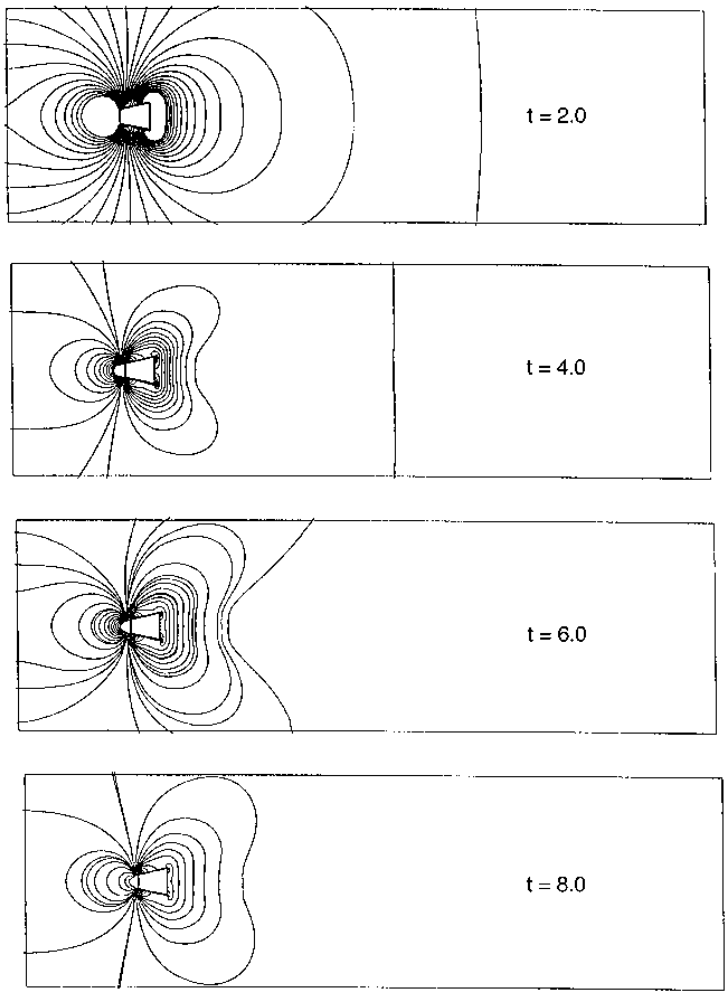

Figure 9.
Time variation of the pressure contours at Re = 25

comparison with the pressure contours for Re = 25 and 50, the outline of the wake region from the frontal corners to the rear stagnation point is larger. From the previous study of the streamline patterns, secondary recirculation is known to develop at these corresponding Reynolds numbers. However, the variations in the pressure contours are not significant when the recirculation regions are fully developed. For higher Reynolds numbers (Figures 12, 13 and 14), the pressure contours become more complex. Separation flow at the frontal corners merge with the recirculation region at the aft end as time advances. The development of the symmetrical eddies at the aft end of the cylinders can be observed from the changes of the pressure contours in the trailing wake region. For Re < 50, the recirculation patterns aft of the cylinder are small. For Re > 250, the pressure contours show complicated patterns

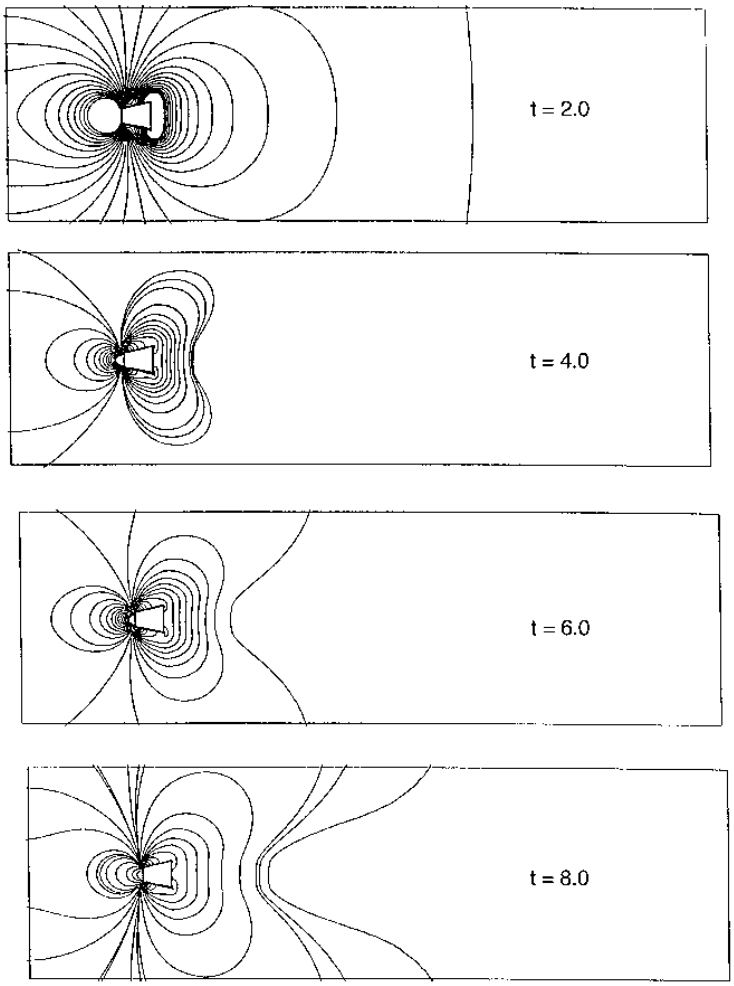

Figure 10.
Time variation of the pressure contours at Re = 50

when compared with that of the lower Reynolds numbers of Re = 25 and 50. At Re = 250, the secondary recirculation region at the upper and lower inclined surfaces of the cylinder can be seen merging with the wake region aft of the cylinder forming a single tertiary recirculating flow region between the separated flow from the leading edge and the recirculation region at the aft end of the cylinder.

Figures 15 and 16 show the distributions of surface pressure coefficients [$Cp = (p - p_\infty)/(0.5\rho_{U\infty}^2)$ at various times for Re = 50 and 500 respectively. Interesting flow features can be observed from these surface pressure coefficients. The surface pressure coefficients at the frontal stagnation point have the maximum positive value. The minimum Cp (negative value) appears on the inclined side

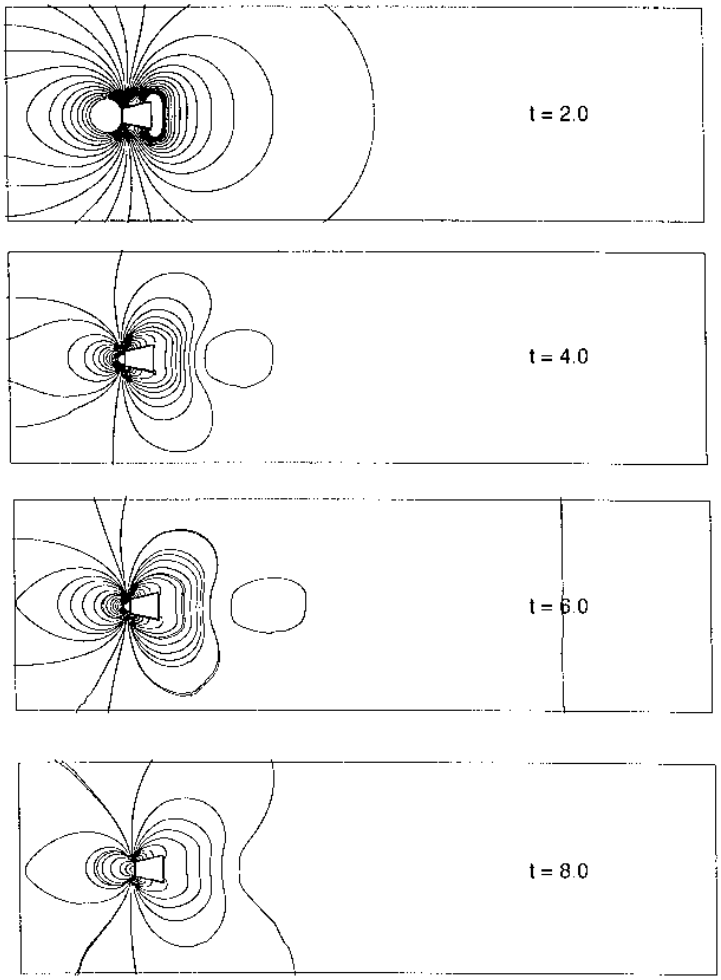

Figure 11.
Time variation of the pressure contours at Re = 150

surfaces immediately after the frontal corners. The changes of the surface pressure coefficients are gradual along the two inclined side walls of the cylinder.

Figure 17 shows the variation of drag coefficients (Cd) with respect to time for the various Reynolds numbers. At low Reynolds numbers, Cd variations exhibit very different patterns from those at high Reynolds numbers. For Re > 250, there is very little variation in the pattern of the Cd. At Re = 25, the initial of the drag coefficient is about 2.9, it drops rapidly as time advances. At t = 6.0, the steady value is about 1.5. For Re = 50 and Re = 150, the drag coefficients show similar trends as those for Re = 25 except the values are much smaller than at Re = 25. For Re > 250, there is no obvious difference between the drag coefficients. In general, at the early time stages, the drag coefficients decrease quickly from the initial maximum value and tend towards a stationary value.

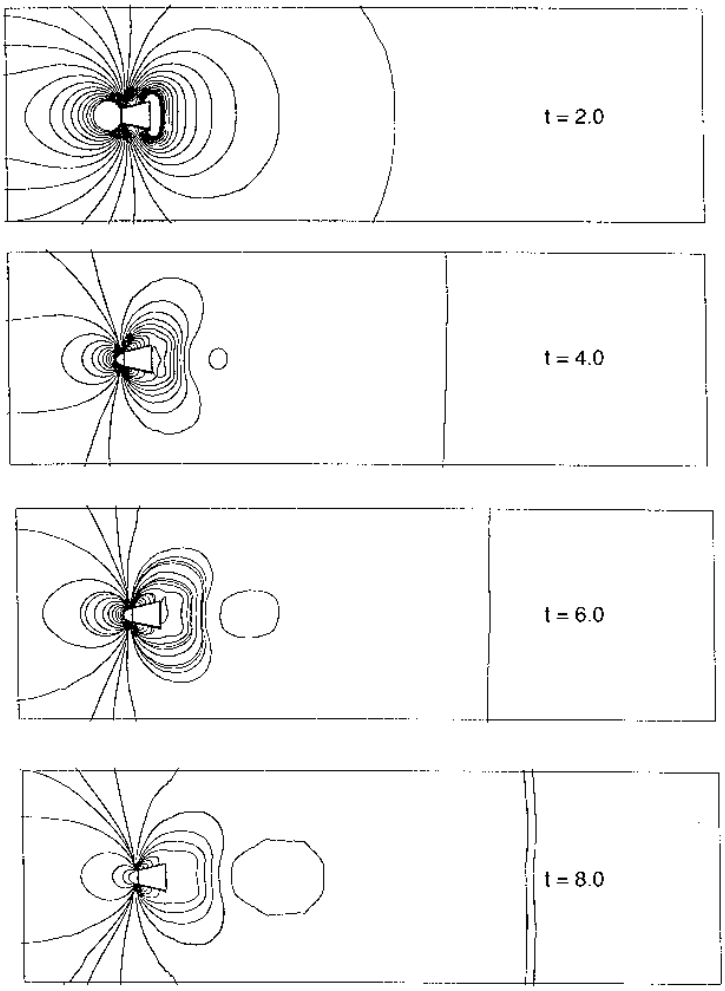

Figure 12.
Time variation of the pressure contours at Re = 250

For Re > 150, there are no obvious differences in the variation of the drag coefficients. For Re = 25, the drag coefficient drops rapidly from its initially maximum value of 2.9. As time advances, Cd varies in a narrow range and the magnitudes of that range become smaller and smaller, and finally after t = 17.0, it approaches a value of approximately 1.50. This is smaller than the corresponding case for square cylinder (Cd = 2.0) under the same flow condition. The Cd-curve for Re = 50 shows similar behaviour. The value is much smaller compared with the case of Re = 25. It approaches a value around 1.40 as time advances. For Reynolds numbers between 150 and 1,000, the Cd curves are similar and the differences between them are small. The drag coefficients decrease rapidly from t = 1.0 to t = 5.0 and then increase after t = 5.0. They soon decrease again at t = 9.0 and eventually approach Cd = 1.50 at t = 18.0. The maximum Cd values

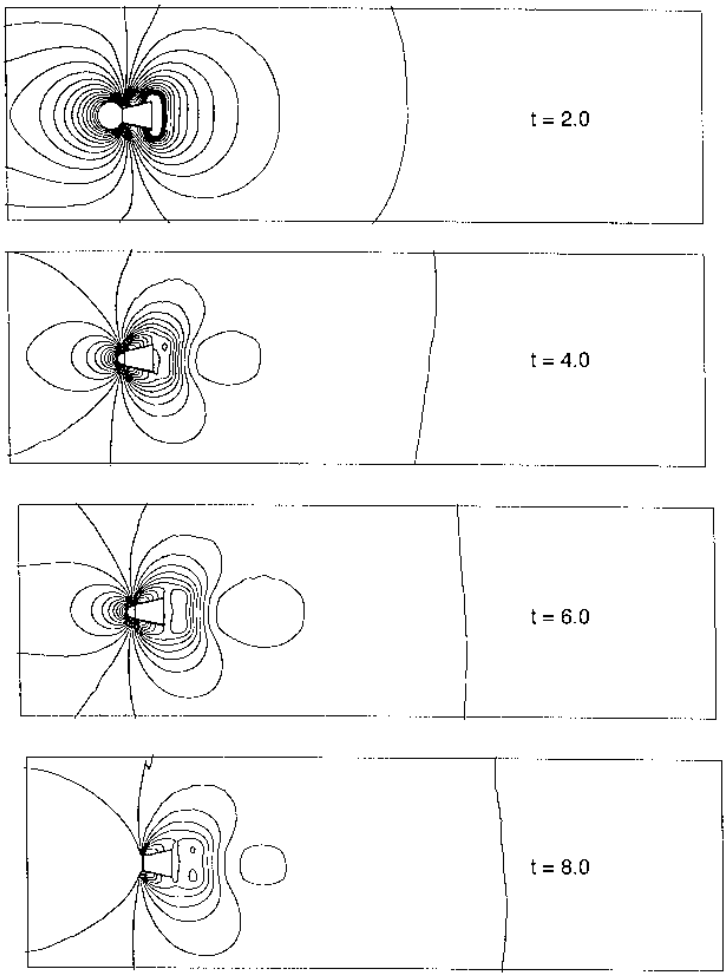

Figure 13.
Time variation of the pressure contours at Re = 500

appear at the beginning of the impulsively started flow over the expanded trapezoidal cylinder. The initial Cd values vary oscillatory owing to the creation of secondary recirculation flow patterns and their changes with respect to the time duration of the initial developmental stages of the impulsively started flow. At the beginning, only the twin vortices appear at the wake region behind the rear wall of the cylinder. The drag decreases from the initial maximum value. When the secondary recirculation is initiated, the drag increases during the developmental stages of the secondary recirculation region. It also takes longer for the drag coefficients to reach steady-state values because of the appearance of the secondary recirculation. In general, the higher the Reynolds number, the smaller the Cd steady-state value. At the early stages of the impulsively started flow, the drag coefficients decrease more rapidly than after some time intervals.

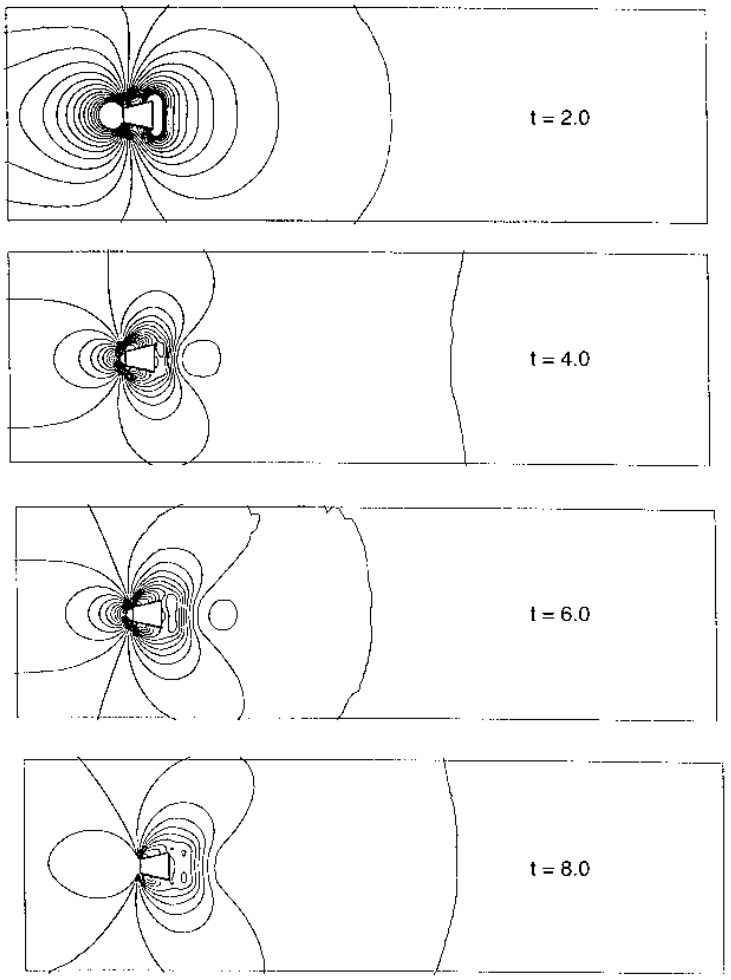

Figure 14.
Time variation of the pressure contours at Re = 1,000

The drag coefficients generally approach a stationary value at large time levels for all the Reynolds numbers considered here.

4. Conclusions

Early stages of an impulsively started laminar flow around an expanded trapezoidal cylinder with $25 < Re < 1{,}000$ were studied numerically. The computed results show that the characteristics of the developing flow recirculation, flow separation and regimes caused by interacting of flows are strongly dependent on the approaching Reynolds number. Four main flow regimes have been identified according to whether: (i) the flows are attached predominantly on to all the surfaces of the cylinder (Type I); (ii) flow recirculation develops at the aft end of the cylinder surface (Type II); (iii) significant flow separation from the leading edges of the cylinder (Type III); (iv)

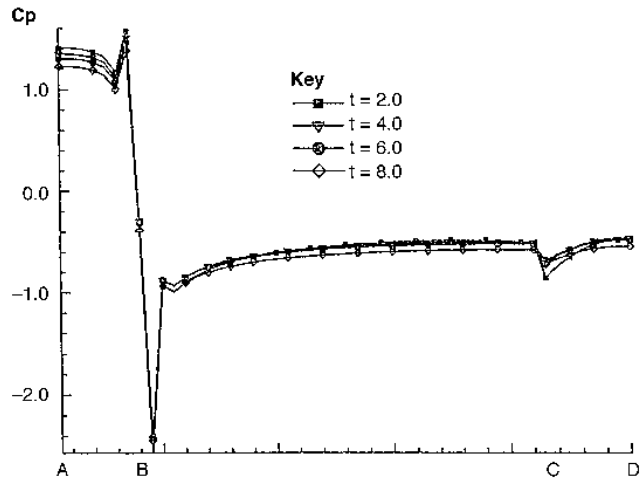

Figure 15.
Time variation of the pressure coefficient at Re = 50

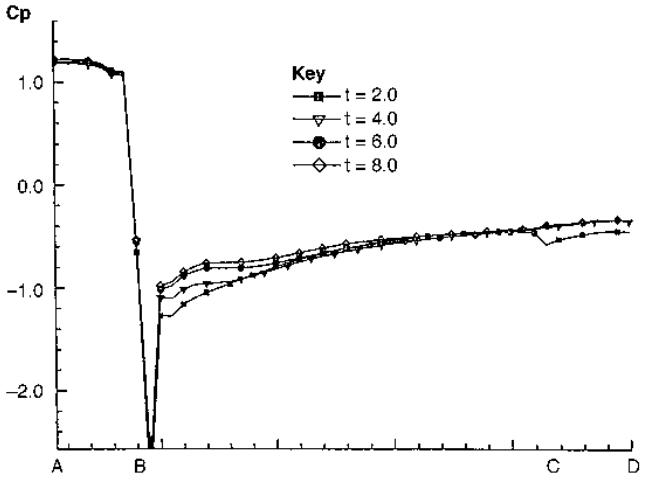

Figure 16.
Time variation of the pressure coefficient at Re = 500

growing of the aft end recirculation zone and the merging with the separating zone of flow from the leading edges; forming a complex tertiary flow phenomena at the boundary of the two main mixing zones (Type IV). Within the Type I-IV main flow characteristics, three significant sub-flow regimes were also identified. Sub-flow (a) shows the growing and development of the symmetrical eddies aft of the cylinder surface; sub-flow (b) identifies the spreading characteristics of the separating shear layer from the leading edges of the cylinder and developing along the inclined surfaces; and sub-flow (c) analyses the complex disturbed flow regime near the meeting point between the developing Type II and Type III flows.

For Re < 25, the initial flow develops with time without visible flow separation (Type I). After a short lapse of time, the flow separates predominantly from the

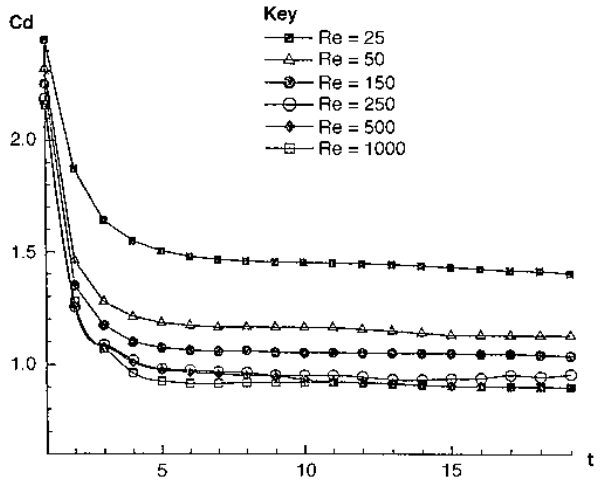

Figure 17.
Time variation of the drag coefficients for various Re

rear surface of the expanded trapezoidal and formed symmetrical eddies within a recirculating zone about the rear axis of the cylinder (Type II). For $25 < Re < 250$, significant secondary phenomena was observed early, namely, the development of a flow separation on the upper and lower inclined surfaces of the expanded trapezoidal cylinder (Type III). For $Re > 250$, the merging of the separation flow (Type III) from the upper and lower inclined surfaces of the cylinder with the recirculation zone of the wake region (Type II) forming the Type IV flow was observed. For a given Re, once Type II and Type III recirculatory flows merged, the overall flow recirculation flow of Type IV flow usually remain fairly constant with the advancement of time.

The time evolution of the various characteristics of the sub-flow regions occur during different phases of the main flow developments. Initially, the primary recirculatory region aft of the cylinder [sub-flow (a)] grow with the width of the wake less than the width of the aft end of the expanded trapezoidal cylinder. As time advances, sub-flow (a) grows wider than the width of the expanded trapezoidal cylinder, and eventually merges with the elongated upper and lower separated surface shear layers [sub-flow (b)] from the leading edges of the cylinder. When sub-flows (a) and (b) merge, complex tertiary sub-flow (c) region develops at the merging point. At this stage, the recirculating zone at the aft end of the cylinder grows wider than the aft width of the cylinder. The length of the separating shear layer from the leading edges grows longer than the length of the cylinder.

References

Bearman, P.W. and Trueman, D.M. (1972), "An investigation of the flow around rectangular cylinders", *Aeronautic Quarterly*, Vol. 23, pp. 229-37.

Bouard, R. and Coutanceau, M. (1980), "The early stage of development of the wake behind an impulsively started cylinder for $40 < Re < 10$", *J. Fluid Mechanics*, Vol. 101 No. 3, pp. 583-607.

Coutanceau, M. and Bouard, R. (1977), "Experimental determination of the main features of the viscous hydrodynamic field in the wake of a circular cylinder in a uniform stream", *J. Fluid Mech.,* Vol. 79, pp. 231-9.

Davis, R.W. and Moore, E.F. (1982), "A numerical study of vortex shedding from rectangles", *J. Fluid Mech,* Vol. 116, pp. 475-506.

Fernando, M.S.U.K. and Modi, V.J. (1990), "A numerical analysis of unsteady flow past bluff bodies", *Computational Mechanics*, Vol. 6, pp. 11-34.

Gerrard, J.H. (1966), "The mechanics of the formation region of vortices behind bluff bodies", *Journal of Fluid Mechanics,* Vol. 25, pp. 401-10.

Gerrard, J.H. (1978), "The wakes of cylindrical bluff bodies at low Reynolds number", *Phil. Trans. Roy. Soc.,* Vol. A 288, pp. 29-38.

Kim, S.W. and Benson, T.J. (1992), "Comparison of the SMAC, PICO and ITERATIVE TIME-ADVANCING schemes for unsteady flows", *International Journal for Numerical Methods in Fluids,* Vol. 21 No. 3, pp. 435-54.

Kyoji, K. and Yoshifumi, Y. (1992), "Observation of the flow around a circular cylinder and a trapezoidal cylinder in a circular pipe by a dye-injection method", *11th Australasian Fluid Mech. Conference,* Vol. 1, 14-18 December, pp. 201-7.

Lisa, M.L. and Balasubramaniam, R. (1993), "Numerical analysis on Strouhal frequencies in vortex shedding over square cylinders with surface suction and blowing", *Int. J. Num. Meth. Heat Fluid Flow,* Vol. 3, pp. 357-75.

Nagano, S. (1982), "A numerical analysis of two-dimensional flow past a rectangular prism by a discrete cortex model", *Computers and Fluids*, Vol. 10 No. 4, pp. 243-59.

Okajima, A. (1982), "Strouhal numbers of rectangular cylinders," *J. Fluid.Mech,* Vol. 123, pp. 379-98.

Okajima, A. and Kitajima, K. (1993), "Numerical study on wake patterns and aerodynamic forces of an oscillating cylinder with a circular and rectangular cross-section", *Journal of Wind Engineering and Industrial Aerodynamics,* Vol. 50, pp. 39-48.

Roache, P.J. (1972), "Computational fluid dynamics", Hermosa Publishers.

Samarskii, A.A. and Andree, V.B. (1963), "On the high accuracy difference scheme for an elliptic equation with several space variables", *USSR Comp. Math. Physics,* Vol. 3, pp. 1373-82.